IEEE Access
Multidisciplinary | Rapid Review | Open Access Journal

Received September 29, 2019, accepted October 31, 2019, date of publication November 4, 2019,
date of current version November 21, 2019.

Digital Object Identifier 10.1109/ACCESS.2019.2951379

A New Phase Sequence Exchanging Control Method for Reducing Impulse Current and Voltage

YIFAN LI[1], SHAOFENG HUANG[1,2], (Member, IEEE), HUI LI[1], JIAN ZHANG[1], GANG HUANG[1], AND YANGJINGYI LUO[1]

[1]State Key Laboratory of Alternate Electrical Power System with Renewable Energy Source, North China Electric Power University, Beijing 102206, China
[2]Beijing Sifang Automation Company Ltd., Beijing 100085, China

Corresponding author: Yifan Li (ivanlee_lyf@163.com)

This work was supported in part by the Beijing Sifang Automation Company Ltd., under Grant KH17010347 and in part by the Fundamental Research Funds for the Central Universities under Grant 2019QN107.

ABSTRACT Phase sequence exchanging technology (PSET) is a recently developed emergency control technology for out-of-step power systems. The PSET system does not satisfy the condition of synchronization however, and will produce impulse current and impact torque. In this paper, the impulse current and impact torque produced by PSET are calculated. Taking the three-phase short circuit at the generator outlet as a reference, the impulse current generated by PSET is determined to be less than half of the three-phase short circuit at the generator outlet, which is within the system's endurable range. When the system connection reactance is 0.543 times larger than generator direct axis sub-transient reactance, it can endure the impact torque produced by PSET. To reduce the impact and improve the practicability of PSET, a split-phase switching control method is proposed in this paper. The characteristics of fast breaking are utilized to turn off the solid-state circuit breaker separately when the three-phase current is at zero-crossing, and after exchanging the phase sequence, it is turned-on separately when two sides of the three-phase voltage are equal. An example is provided to verify that the impact of PSET can be dramatically reduced by using the proposed control method instead of the traditional simultaneous switching control method.

INDEX TERMS Phase sequence exchange technology, impulse current, impact torque, split-phase switching control method.

I. INTRODUCTION

The continuous expansion of the power system is creating an increasingly complex power grid structure [2]–[4]. This is further complicated by emerging inter-regional tie lines and long-distance large-capacity transmission systems. Due to environmental and economic constraints, the system operates at a level close to the stability limit state, meaning that maintaining the security and stability of the power system is increasingly serious [5]–[10]. Due to the emerging electricity market, additional changes are predicted to occur in the operation mode and conditions of the power grid, making its dynamic behavior increasingly complex [11].

Emergency control systems are an effective measure to improve system stability and the ensure safe and stable operation of the power grid [12]–[18]. Such procedures can take control of the power system in a disturbance emergency to prevent the system from compromising stability or exceeding operating parameters, as well as further expansion of the accident which could lead to widespread blackouts [19]. Emergency control can also improve the transmission power of some transmission lines in which capacity is limited by transient stability limit, and even boost the transmission power of lines close to the static stability limit [20]–[22]. In the modern power system, the purpose of emergency control decision making is to determine control measures which can stabilize the system and minimize costs under given faults.

Reference [1] presented a recently developed emergency control method, phase sequence exchange technology (PSET). This technique utilizes controllable power electronic components to form a phase sequence exchanging device,

The associate editor coordinating the review of this manuscript and approving it for publication was Lin Zhang.

taking the system power angle as a control variable to realize a series of functions including fast interruption, phase sequence adjusting, and fast closing at the appropriate time. Phase sequence exchange technology can prevent a system from becoming out-of-step, while still maintaining the structural integrity of the power grid. As detailed in [1], the PSET process begins when the power electronic device, consisting of solid state circuit breakers, disconnects the line. The phase sequence is then exchanged in turn, and the solid state circuit breaker is activated. However, after switching, the power angle of the system does not usually satisfy the condition of synchronization when the solid state circuit breaker is activated. Thus, impulse current and torque will inevitably occur in the closing process [23]–[26]. Impulse current can destroy the generator, terminate the electrical performance of the power system, and burn generator windings in serious cases. Additionally, the impact current can produce tremendous stress on the stator end winding of the generator, destroying the winding itself. The impact of electromagnetic torque can also produce strong torsional stress, which will cause fatigue loss in the torsional vibration of the system, shorten the service life of the shaft, and potentially lead to immediate fracture of the generator shaft [27]–[34]. In [27], it was determined that asynchronous closing can be carried out when there is enough contact reactance between two parts of the power system. It is therefore necessary to calculate and verify the impact caused by PSET, and to verify the "cost" of the phase sequence exchanging operation. Once this is determined, the appropriate control mode can be adopted to return the system to synchronization with minimum impact on the system.

The main contributions of this paper are as follows:

1. The impulse current and impact torque produced by PSET are calculated

2. The impulse current produced by PSET is determined as less than half of the three-phase short-circuit current at the generator outlet, thus the power grid can withstand it.

3. The conditions under which the system can withstand the PSET impact torque are calculated.

4. A control method to reduce the impact of PSET is proposed.

5. An example is provided to verify the effectiveness of the control method.

The remainder of this paper is organized as follows: Section II briefly introduces the phase sequence exchange technology. In Section III, the impulse current and impact torque generated by the PSET is calculated, and the conditions under which the system can withstand the impulse of PSET are provided. A split-phase switching control method of turning-off at the zero-crossing point of current and turning-on at the equal voltage control is proposed in Section IV to reduce the impact of PSET on the system. Section V verifies the effectiveness of the control method by actual system simulation, and concluding remarks are provided in Section VI.

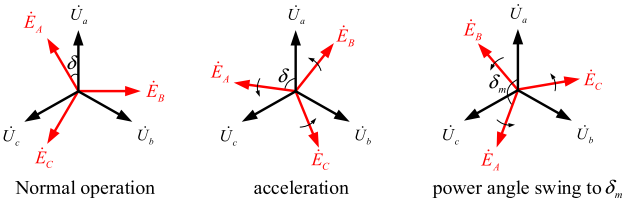

FIGURE 1. Three-phase power angle vector diagram.

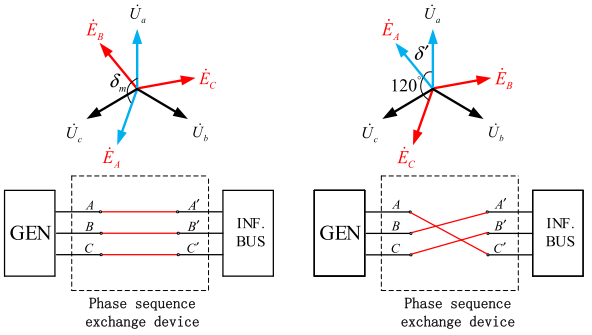

FIGURE 2. Vector diagram and phase sequence connection diagram of phase A.

II. INTRODUCTION OF PHASE SEQUENCE EXCHANGE TECHNOLOGY

Phase sequence exchange technology (PSET) is a recently developed power system emergency control method which can be used to prevent the system from entering an out-of-step condition. In a case such as a one-machine-to-infinite-bus system that has experienced disturbance in which the power angle has swung to a certain angle between 90°–180°, PSET can be used. The power angle threshold of PSET is set to δ_m. When the system is out-of-step and the power angle swings to δ_m, using power electronic equipment quickly misaligns the connection by disconnecting the primary side phase of the contact line. The A, B, C three-phase sequence then connects to the three-phase C, A, B sequence, instantaneously reducing the angle by 120°, thus restraining the system from entering the out-of-step condition. A power angle vector diagram illustrating this process is provided in Fig. 1.

In a situation in which the phase sequence exchange is $\delta = \delta_m$, the following steps must be followed. Take phase A, where the power angle δ_A before the phase sequence exchange is the angle between phasor $\dot{E}_A$ and $\dot{U}_a$. After the phase sequence exchange, the power angle δ_A is the angle between the phasor $\dot{E}_B$ (which is changed to $\dot{E}_A$ after the phase sequence exchange) and $\dot{U}_a$. A vector diagram of phase A and a phase sequence connection diagram are provided in Fig. 2, where it can be seen that the phase sequence exchange reduces the power angle of the system by 120°.

III. THE IMPACT OF PHASE SEQUENCE EXCHANGE TECHNOLOGY

This section verifies the feasibility of the commutation sequence operation from the two aspects of impulse current

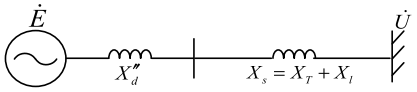

FIGURE 3. One-machine-to-infinite-bus model.

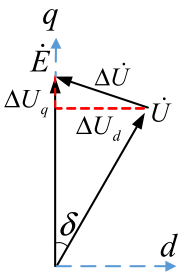

FIGURE 4. Voltage phasor diagram at turning-on.

and impulse torque. The most serious fault is the three-phase short circuit at the generator outlet, which is used as the calibration benchmark. If the impulse current and torque caused by the commutation sequence are less than those caused by the three-phase short circuit at the generator outlet, the impact caused by commutation sequence can be considered within the endurable range of the system.

A. IMPULSE CURRENT CALCULATION

A one-machine-to-infinite-bus model is used for analysis in this paper, as shown in Fig. 3. In this model, $\dot{E}$ is the generator no-load potential, $\dot{U}$ is the infinite bus voltage, X''_d is the generator direct axis sub-transient reactance, and X_s is the system connection reactance, including transformer reactance X_T and line reactance X_l. The loop resistance is neglected in the analysis process.

The voltage phasor diagram at closing is shown in Fig. 4. Here, $\Delta\dot{U}$ is the relative difference between the generator potential $\dot{E}$ and infinite bus voltage $\dot{U}$ when activated, while ΔU_d and ΔU_q are the projections of $\Delta\dot{U}$ on D and Q axes, respectively. Due to $\Delta\dot{U} \neq 0$, impulse current will be generated during closing.

According to Fig. 4, it can be determined that:

$$\begin{cases} \Delta U_d = -U \sin\delta \\ \Delta U_q = E - U\cos\delta \end{cases} \tag{1}$$

The d and q axis components of the impulse current are:

$$\begin{cases} I_d = \dfrac{-U\sin\delta}{X''_d + X_s} \\ I_q = \dfrac{E - U\cos\delta}{X''_q + X_s} \end{cases} \tag{2}$$

Therefore, the magnitude of the impulse current is:

$$I = \sqrt{I_d^2 + I_q^2} = \sqrt{\left(\frac{U\sin\delta}{X''_d + X_s}\right)^2 + \left(\frac{E - U\cos\delta}{X''_q + X_s}\right)^2} \tag{3}$$

Assuming $X''_d = X''_q$ and $E = U$, Eq. (3) can be simplified as follows:

$$I = \frac{U}{X''_d + X_s}\sqrt{\sin^2\delta + (1-\cos\delta)^2} = \frac{2U\sin\frac{\delta}{2}}{X''_d + X_s} \tag{4}$$

B. CONDITIONS TO WITHSTAND IMPULSE CURRENT

When $\delta = 180°$, the impulse current generated by closing (without considering the aperiodic component) reaches the maximum, which is about $2U/\left(X''_d + X_s\right)$. In practical application, phase sequence exchanging must be achieved before the power angle reaches 180°. Assuming the exchange phase sequence is $\delta = 150°$, the power angle of the system is $\delta = 30°$ when activated, and the current value obtained is far less than that in the most serious case. Substituting $\delta = 30°$ to Eq. (4), the impulse current is approximately $0.52U/\left(X''_d + X_s\right)$.

Based on the impulse current generated by the three-phase short circuit at the generator outlet, the impulse current created by PSET is then analyzed to determine if the system can withstand the impulse current. The initial periodic component current $I_k^{(3)}$ of the generator terminal when three-phase short circuit suddenly occurs is:

$$I_k^{(3)} = \frac{E''_d}{X''_d} \tag{5}$$

The ratio of the impulse current caused by PSET to the impulse current caused by the three-phase short circuit at the outlet is defined as k:

$$k = \frac{I}{I_k^{(3)}} = \frac{0.52U/(X''_d + X_s)}{E''_d/X''_d} \tag{6}$$

Assuming $U = 1.0$ and $E''_d = 1.05$, then k is:

$$k = \frac{0.5}{1 + X_s/X''_d} \tag{7}$$

According to Eq. (7), as $X_s/X''_d > 0$, then $k < 0.5$ is always valid, that is, the impulse current caused by PSET is less than half of the three-phase short circuit current at the outlet. Therefore, it is concluded that the impulse current caused by PSET is far worse than that caused by the three-phase short circuit at the generator outlet.

As stated in [27], when considering the impact of impulse current produced by asynchronous closing on the generator, the electromotive force produced by the current at the end of stator winding must be less than half of the electromotive force produced by the three-phase sudden short circuit. That is to say, the impulse current under asynchronous closing is less than $1/\sqrt{2}$ of the three-phase short circuit current. It can be clearly seen from Eq. (7) that the impulse current caused by PSET satisfies the relationship numerically. Therefore, it is concluded that the impulse current generated by PSET is acceptable to the system.

C. IMPACT TORQUE CALCULATION

Applying the superposition principle, the turning-on process of PSET can be seen as a sudden series of voltage sources at

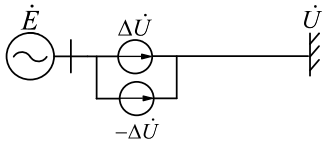

FIGURE 5. Schematic diagram of superposition principle.

the break of the solid state circuit breaker, which are equal to the break voltage before closing and opposite in direction. A schematic diagram illustrating this principal is provided in Fig. 5.

Before turning-on, the voltage difference between the generator potential $\dot{E}$ and the infinite bus voltage $\dot{U}$ is $\Delta\dot{U}$; the closing process is considered a sudden series of voltage sources $-\Delta\dot{U}$ at the break, and the superimposed power source $-\Delta\dot{U}$ acts on the generator in the non-excitation state (i.e., zero initial state). The essential principal of calculating impulse electromagnetic torque is to analyze the additional current and flux linkage generated by the stator loop under the action of superimposed power supply, and to add them to the stator current and flux linkage before turning-on. This will provide the current and flux linkage of the stator loop immediately after turning-on. The final closing impulse torque is calculated according to Eq. (8).

$$\begin{aligned} T_e &= i_q\psi_d - i_d\psi_q \\ &= (i_{q|0|}+\Delta I_q)(\psi_{d|0|}+\Delta\psi_d)-(i_{d|0|}+\Delta I_d)(\psi_{q|0|}+\Delta\psi_q) \end{aligned} \tag{8}$$

where $i_{d|0|}$, $i_{q|0|}$, $\psi_{d|0|}$, $\psi_{q|0|}$ are the d and q components of stator current and flux linkage before closing, respectively,ΔI_d, ΔI_q are the d and q axis current caused by superimposed power supply, and $\Delta\psi_d$, $\Delta\psi_q$ are the d and q axis flux caused by superimposed power supply.

The analogical Eq. (1) decomposes the superimposed power $-\Delta\dot{U}$ into d and q axes, providing:

$$\begin{cases} -\Delta U_d = U\sin\delta \\ -\Delta U_q = U\cos\delta - E \end{cases} \tag{9}$$

The Laplace operation form of the basic voltage and flux equation of synchronous machine can be written as [39]:

$$\begin{cases} U_d(p) = -rI_d(p)+[p\psi_d(p) - \psi_{d0}] - \psi_q(p) \\ U_q(p) = -rI_q(p)+\left[p\psi_q(p) - \psi_{q0}\right]+\psi_d(p) \\ \psi_d(p) = -X_d(p)I_d(p)+G_f(p)\left[U_f(p)+\psi_{f0}\right]+G_D(p)\psi_{D0} \\ \psi_q(p) = -X_q(p)I_q(p)+G_Q(p)\psi_{Q0} \end{cases} \tag{10}$$

Eq. (10) is an image functional equation containing only stator variables and excitation voltage. The detailed meaning of each variable can be found in reference [39]. As the superimposed power acts on the generator without excitation, the Laplace equation of superimposed components can be written in the following form (ignoring stator resistance):

$$\begin{cases} -\Delta U_d/p = p*\Delta\psi_d(p) - \Delta\psi_q(p) \\ -\Delta U_q/p = p*\Delta\psi_q(p) + \Delta\psi_d(p) \\ \Delta\psi_d(p) = -X_d(p)\Delta I_d(p) \\ \Delta\psi_q(p) = -X_q(p)\Delta I_q(p) \end{cases} \tag{11}$$

where $-\Delta U_d$ and $-\Delta U_q$ are the d and q axis components of the superimposed power supply $-\Delta\dot{U}$, respectively, while $\Delta\psi_d(p)$ and $\Delta\psi_q(p)$ are the image functions of the d and q axis flux linkage caused by the superimposed power supply. Subscript $\Delta I_d(p)$ and $\Delta I_q(p)$ are image functions of d and q axis currents caused by superimposed power supply, respectively, $X_d(p)$ and $X_q(p)$ are the calculating reactance of the straight axis and quadrature axis. When $t = 0$, $X_d(p)$ and $X_q(p)$ are equal to X''_d and X''_q of the straight axis and quadrature axis subtransient reactance. If the system connection reactance is taken into account, X''_d and X''_q can be replaced by $X''_d + X_s$ and $X''_q + X_s$.

The unknowns in Eq. (11) are $\Delta\psi_d(p)$, $\Delta\psi_q(p)$, $\Delta I_d(p)$ and $\Delta I_q(p)$, and the number of equations and unknowns is four. Solving the equation provides:

$$\begin{cases} \Delta I_d(p) = \dfrac{p\Delta U_d + \Delta U_q}{p(1+p^2)X_d(p)} \\ \Delta I_q(p) = \dfrac{-\Delta U_d + p\Delta U_q}{p(1+p^2)X_q(p)} \\ \Delta\psi_d(p) = -\dfrac{p\Delta U_d + \Delta U_q}{p(1+p^2)} \\ \Delta\psi_q(p) = \dfrac{\Delta U_d - p\Delta U_q}{p(1+p^2)} \end{cases} \tag{12}$$

The inverse Laplacian transformation of Eq. (12) is carried out, and the time domain analytical formula is obtained.

$$\begin{cases} \Delta I_d = \dfrac{\Delta U_d * \sin\delta_e + \Delta U_q * (1-\cos t)}{X''_d + X_s} \\ \Delta I_q = \dfrac{\Delta U_d * (\cos\delta_e - 1) + \Delta U_q * \sin\delta_e}{X''_q + X_s} \\ \Delta\psi_d = -\Delta U_d * \sin\delta_e + \Delta U_q * (\cos\delta_e - 1) \\ \Delta\psi_q = \Delta U_d * (1-\cos\delta_e) - \Delta U_q * \sin\delta_e \end{cases} \tag{13}$$

By substituting the d and q axis components of superimposed power supply in Eq. (9) into Eq. (13), the time domain analytical expressions of current and flux caused by superimposed power supply are determined.

$$\begin{cases} \Delta I_d = \dfrac{U\left[\cos(\delta+\delta_e) - \cos\delta\right] + E(1-\cos\delta_e)}{X''_d + X_s} \\ \Delta I_q = \dfrac{U\left[\sin\delta - \sin(\delta+\delta_e)\right] + E\sin\delta_e}{X''_q + X_s} \\ \Delta\psi_d = U\left[\cos\delta - \cos(\delta+\delta_e)\right] + E(\cos\delta_e - 1) \\ \Delta\psi_q = U\left[\sin(\delta+\delta_e) - \sin\delta\right] - E\sin\delta_e \end{cases} \tag{14}$$

The expressions of the d and q axis components of current and flux caused by superimposed power supply are shown in Eq. (14).

Before activation, the generator is in a no-load operation state, and $i_{d|0|} = i_{q|0|} = 0$, $\psi_{d|0|} = E$ and $\psi_{q|0|} = 0$.

By substituting the current caused by the superimposed power supply in Eq. (14), as well as the flux linkage and the current and flux linkage in the initial state of the generator before closing into Eq. (8), the final expression of the electromagnetic torque at closing can be obtained.

$$\begin{aligned} & T_e \\ & = (i_{q|0|}+\Delta I_q)(\psi_{d|0|}+\Delta\psi_d)-(i_{d|0|}+\Delta I_d)(\psi_{q|0|}+\Delta\psi_q) \\ & = E^2\left[\frac{1}{X''_d+X_s}\sin\delta_e-\frac{1}{2}\left(\frac{1}{X''_d+X_s}-\frac{1}{X''_q+X_s}\right)\sin 2\delta_e\right] \\ & \quad +U^2\left(\frac{1}{X''_d+X_s}-\frac{1}{X''_q+X_s}\right) \\ & \quad \times\left[\sin(\delta_e+2\delta)-\frac{1}{2}\sin 2\delta-\frac{1}{2}\sin 2(\delta_e+\delta)\right] \\ & \quad +UE\left\{\left(\frac{1}{X''_d+X_s}-\frac{1}{X''_q+X_s}\right)\right. \\ & \quad \left.\cdot[\sin(\delta_e+2\delta)-\sin(\delta_e+\delta)]\right. \\ & \quad +\frac{1}{X''_d+X_s}[\sin\delta-\sin(\delta_e+\delta)] \end{aligned} \tag{15}$$

In Eq. (15), E is the no-load potential of the generator, U is the system side voltage, δ is the power angle when closing, and δ_e is the angle experienced after closing. The generator rotor slip is neglected in this formula, that is to say, the generator speed is at speed ω_0 when it is activated. In fact, the speed of the generator is not ω_0 at this time, however, when calculating impact torque, neglecting the speed deviation of 5%∼10% does not affect the final calculation result.

D. CONDITIONS TO WITHSTAND IMPULSE TORQUE

Eq. (15) is the expression of impulse torque which ignores the generator slip. Assuming that the vertical and quadrature sub-transient reactances are equal, that is $X''_d = X''_q$, a simplified electromagnetic torque expression can be obtained:

$$T_e = \frac{E^2}{X''_d+X_s}\sin\delta_e+\frac{UE}{X''_d+X_s}[\sin\delta-\sin(\delta_e+\delta)] \tag{16}$$

If the generator no-load potential E is 1.2 and the system side voltage U is 1.0, the combined formula (3-16) is as follows:

$$T_e = \frac{1.44}{X''_d+X_s}\sin\delta_e+\frac{1.2}{X''_d+X_s}[\sin\delta-\sin(\delta_e+\delta)] \tag{17}$$

After phase sequence exchanging, the power angle of the system is reduced by 120°, assuming that the power angle of the system is in the range of 20° to 60° when the system is activated. Fig. 6 provides an image of the electromagnetic torque function in a power frequency cycle after activation as according to equation. (17).

According to Fig. 6, the maximum electromagnetic torque appears at $\delta = 60°$, $\delta_e = 146.9°$, and the maximum torque value is approximately $2.369/(X''_d + X_s)$. That is to say, when the power angle is 60°, and turning 146.9° electric angle after turning-on, the electromagnetic torque reaches its peak value, that is, the impact torque produced by PSET is $T_e|_{\max} = 2.369/(X''_d + X_s)$.

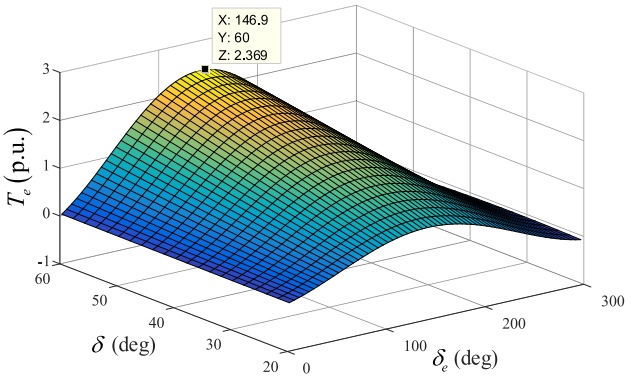

FIGURE 6. Variation of electromagnetic torque T_e with power angle δ and electric angle δ_e after activation.

The impact torque generated by the three-phase short-circuit at the generator outlet is still taken as a reference to analyze the impact torque tolerance capacity of the system. The three-phase short circuit at the outlet is equivalent to the sudden closing of the generator in the zero potential system. Therefore, $U = 0$, $X_s = 0$ is substituted for Eq. (16) to obtain the electromagnetic torque $T_{ek}^{(3)}$ of the three-phase short circuit at the outlet:

$$T_{ek}^{(3)} = \frac{E''^2_d}{X''_d}\sin\delta_e \tag{18}$$

where E''_d is the transient potential of the short circuit, and is usually 1.05. Obviously, when $\delta_e = 90°$, which is 1/4 cycle after activation, the electromagnetic torque reaches the maximum $T_{ek}^{(3)}|_{\max} = 1.103/X''_d$.

Taking the three-phase short circuit at the outlet as a reference, the impact torque produced by PSET must be less than that produced by the short circuit. That is:

$$T_e|_{\max} < T_{ek}^{(3)}|_{\max} \tag{19}$$

Eq. (17) and Eq. (18) are then introduced into Eq. (19), providing the following:

$$\frac{X_s}{X''_d} > 0.543 \tag{20}$$

When the contact reactance X_s is greater than 0.543 times that of the generator's straight axis sub-transient reactance X''_d, the impact torque caused by PSET is less than that caused by the three-phase short circuit at the outlet.

The contact reactance of the system mainly depends on the transformer and the line. When the contact reactance of the system does not satisfy Eq. (20), the system cannot withstand the impact torque caused by PSET. In order to satisfy Eq. (20), the contact reactance of the system can be increased by splitting the winding transformer and installing a current limiting reactor to satisfy the application conditions of PSET. However, the excessive contact reactance of the system will reduce the static stability and power limit of the system,

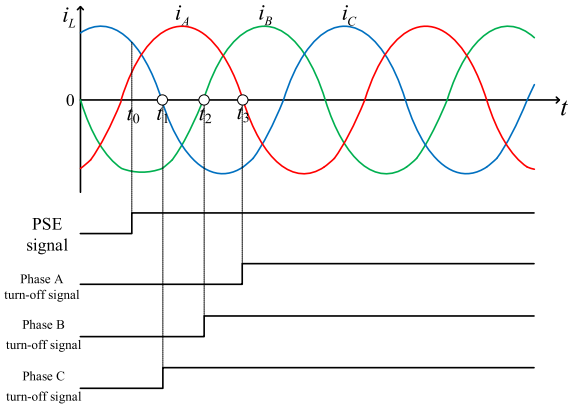

FIGURE 7. opening when current zero-crossing.

as well as weaken the anti-disturbance ability. Therefore, it is necessary to assess advantages and disadvantages in order to reduce the impact torque. The contact reactance is usually 0.543 times larger than the direct-axis transient reactance of the generator. Thus, the general power system can withstand the impact torque caused by PSET.

IV. A CONTROL METHOD TO REDUCE THE IMPACT OF PSET

In the process of phase sequence exchanging, the opening and closing operation of the solid state circuit breaker (SSCB) will create overvoltage and overcurrent in the power system, reducing the stability of system operation, and posing a large safety risk to high-voltage transmission lines and power equipment [35],[36]. In the previous section, a splitting winding transformer and current limiting reactor were proposed to increase the contact reactance of the system to reduce the impact of PSET. However, the excessive contact reactance of the system will affect its transient stability. In this section, a control method to reduce the impact of PSET is put forward.

When the voltages on both sides of the system are equal, the turn-on current is the smallest [37],[38]. Based on this condition, a split-phase switching control method is proposed. After the SSCB receives the phase sequence exchanging command, the real-time values of voltage and current are obtained by sampling. When the currents of the three phases respectively cross the zero point, the three-phase SSCB is turned off in turn. After the three phases are completely turned off, the phase sequence is exchanged and a signal is sent to allow system activation. The voltage across the SSCB is then compared, and when it is equal, the system can be activated and the phase sequence exchange is complete.

The connection mode before the system is shut off ahead of phase sequence exchanging is illustrated in Fig. 2. The current i_A of phase A is the current from A to A'. Fig. 7 shows a schematic diagram of opening with current zero-crossing. The red, green, and blue curves in Fig. 7 respectively represent i_A, i_B and i_C of the three-phase current. Subscripts t_1, t_2 and t_3 are the first zero crossing of three-phase current i_C, i_A and i_B after receiving the phase sequence exchange signal (PSE signal) at t_0. As the SSCB has a fast breaking speed and

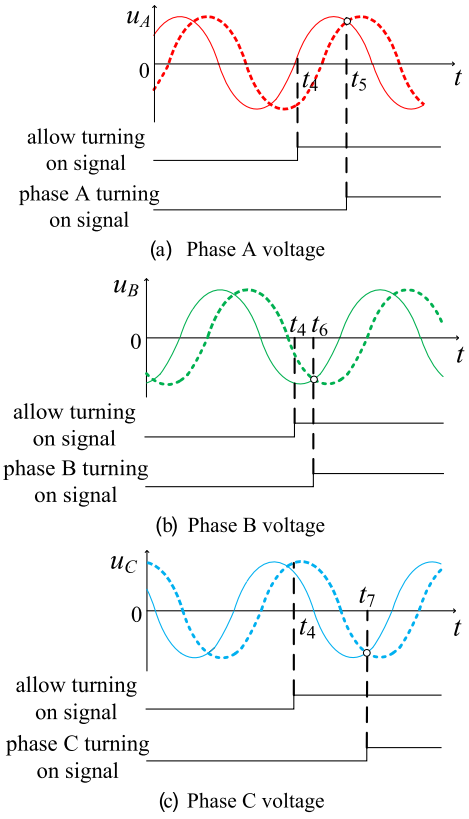

FIGURE 8. Phase separation activation diagram.

can achieve precise control, it can be opened at the time when the phase currents cross the zero point, in which the surge voltage to the system is minimized. The real-time change of the current is determined by sampling the instantaneous value of the current through the current transformer. In Fig. 7, the earliest zero-crossing point of C-phase current is monitored and the C-phase shut off signal is sent out. The other two phases are analogous, and the current transformer continues to monitor the current of A and B phases. When the current crosses zero point, the system shut off signal is sent to turn off the three-phase split-phase.

When all three phases are turning-off, zero-crossing voltage should be detected. According to the system connection diagram following phase sequence exchanging in Fig. 2, the voltage u_A of phase A after phase sequence exchanging is the voltage difference between the A phase of the original generator and the C' phase of the system. The voltage u_B of phase B after phase sequence exchanging is the voltage difference between the B phase of the original generator and the A' phase of the system. The voltage u_C of phase C after phase sequence exchanging is the voltage difference between the C phase of the original generator and the B' phase of the system.

A schematic diagram of the equal-pressure activation process is provided in Fig. 8. The solid line in the figure is the voltage waveform on the left side (generator) of the SSCB, and the right-dashed line is the voltage waveform on the right

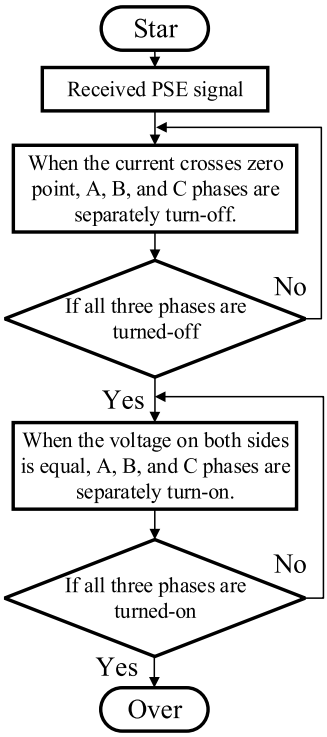

FIGURE 9. Flow chart of the control method.

side (system) of the SSCB. The three diagrams a), b), and c) in Fig. 8 respectively illustrate the three-phase turning on situation of a, b, and c. The closing action of the SSCB is controlled by the comparison of voltages on both sides of the SSCB.

As shown in Fig. 8, after the allowable activation signal is issued at time t_4, the voltage on the left and right sides of phase B first reach the same value, then the switch on signal is issued to complete activation. Phase A and phase C are then activated in sequence after reaching the switching on condition. The three phases then complete activation and the phase sequence is exchanged.

This control method requires the instantaneous value of voltage and current in the process of turning-on and turning-off, however, it can be utilized selectively according to the operating conditions, resulting in less system impact and superior performance.

A split-phase switching control method is proposed in this section which utilized the characteristics of fast breaking of the solid-state circuit breaker for shutting off at the zero-crossing point of current and activating when two sides of the three-phase voltage are equal. The impact of PSET can be reduced through the control mode of split-phase activation and shutting off.

The flow chart in Fig. 9 summarizes the proposed control method.

In short, any phase is shut off when the current equals zero, exchange phase sequence after the three phases are shut off, and any phase are switched on when the voltage equals zero.

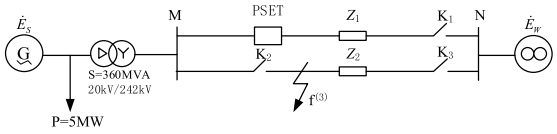

FIGURE 10. OMIB model.

V. A SIMULATION TEST

A. POWER SYSTEM MODEL

Simulink was used to build a simulation model to verify the effectiveness of the control method proposed in the previous section. The one machine infinite bus (OMIB) system model was utilized in the simulation, as shown in Fig. 10.

Generator terminal voltage was 20 kV, run through a 20 kV/242 kV transformer and a 110 km double-circuit transmission line connected with a 220 kV infinite bus system. The relevant parameters of the system were as follows transformer capacity 360 MVA; impedance of the transmission line $x_0 = 0.89145$ (Ω/km); $x_1 = 0.32578$ (Ω/km); $c_0 = 8.257 \times 10^{-9}$ (F/km); $c_1 = 11.2567 \times 10^{-9}$ (F/km); $r_0 = 0.22131$(Ω/km); $r_1 = 0.03921$(Ω/km). The parameters of the double circuit lines were the same, that is $Z_1 = Z_2$.

B. SIMULATION ANALYSIS

To reduce the impact of PSET, a control method is proposed in which the solid-state circuit breaker is applied to PSET for switching off separately at the zero-crossing point of three-phase current and activating separately when there is equal voltage on both sides. To verify the control effect of split-phase switching, the control methods of three-phase simultaneous switching are compared in this section.

In the simulation, the initial state of single machine infinite bus system is stable, and a three-phase short-circuit fault occurs at the beginning of loop II at 0.1 s. After the fault lasts for 0.2 s, the fault line is removed and the system changes from double-loop operation to single-loop operation. Because of the serious short-circuit fault, the power transmission between the generator and system side is unbalanced, the generator rotor accelerates, and the system is unstable. The wave of rotor speed, power angle, three-phase voltage, and current waveforms are provided in Fig. 11 (a), (b), (c), and (d), respectively.

Fig. 11 (a) shows the speed of the generator rotor. It can be observed from the figure that the speed of the generator rotor is stable at the rated speed before the short circuit. The speed then rises linearly after the short circuit, and rises in fluctuation after the fault is removed. Each fluctuation is accelerated and then decelerated, and the overall trend of acceleration is still present.

Fig. 11 (b) shows the power angle of the system. Before the fault, the power angle of the system is 46.3°. After the fault, the power angle oscillates between 0° and 360°, and the frequency of the first few cycles is slower. As the rotor accelerates, the oscillation time becomes longer and the frequency becomes faster.

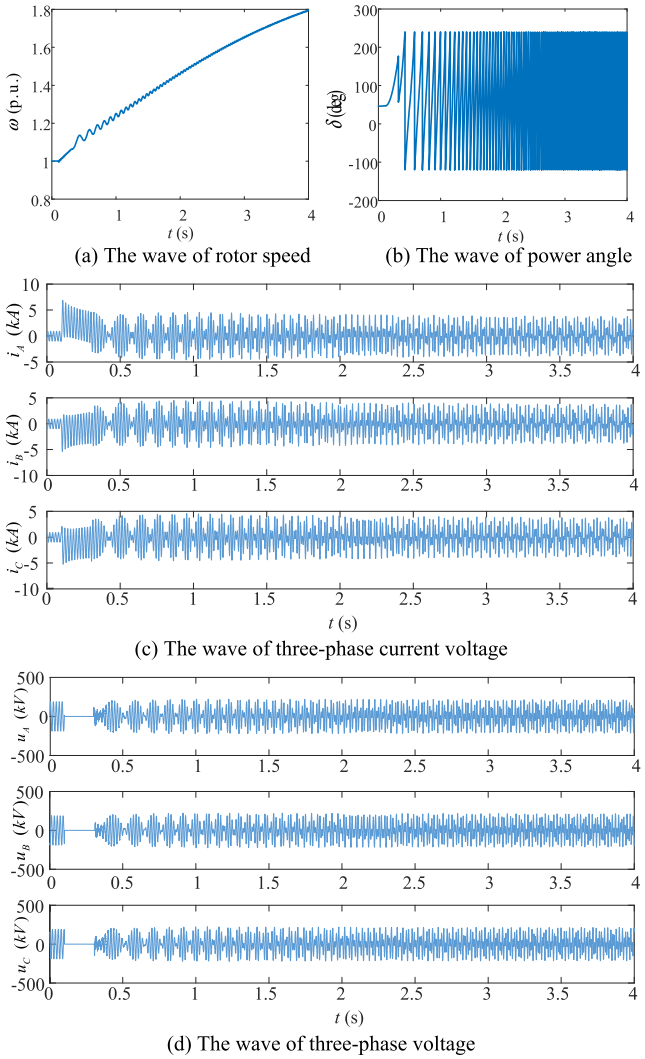

FIGURE 11. System simulation waveform without emergency control.

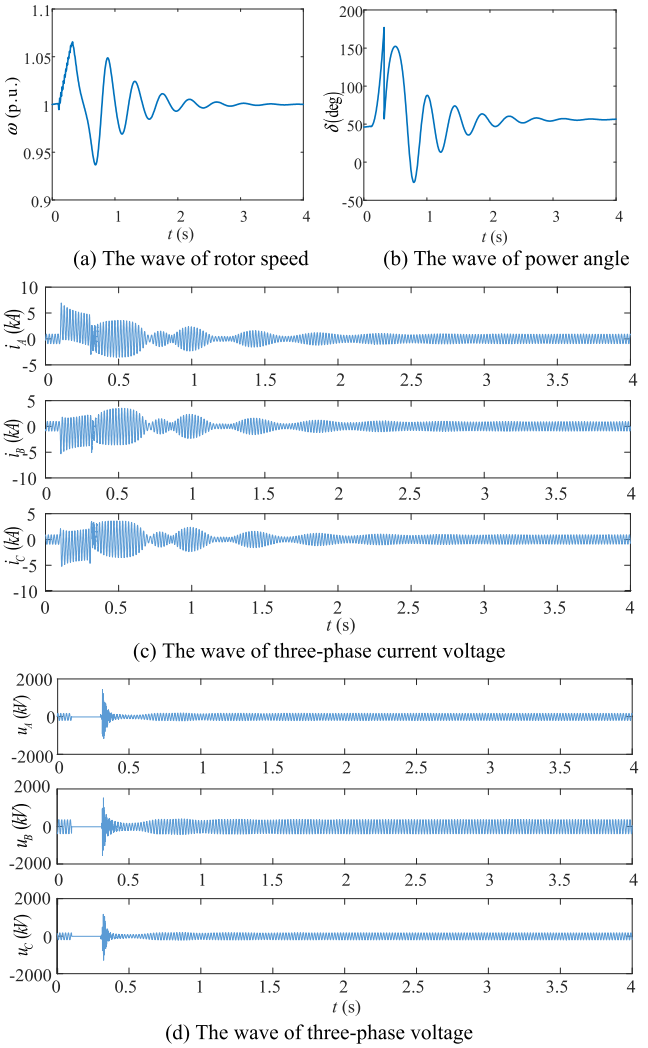

FIGURE 12. System simulation waveform with synchronous switching control method.

Fig. 11 (c) shows the three-phase current of the line. Before the fault is removed, the three-phase current increases sharply. After the fault is removed, the three-phase current begins to oscillate, the amplitude changes sinusoidally, and the frequency difference between the two sides of the system is the frequency difference. The maximum amplitude can reach two-thirds of the three-phase short-circuit current.

Fig. 11 (d) shows the three-phase ground voltage on the generator side, which changes to zero when the short-circuit occurs. When the fault line is removed, the voltage waveform appears at peak overvoltage, then the amplitude of the waveform changes sinusoidally with the frequency difference between the two sides of the system.

Due to the late removal of the fault, the system experiences a loss of synchronism. In this case, PSET is used to prevent the system entering an out-of-step condition. In this simulation, a solid state circuit breaker is used realize the PSET.

A three-phase short-circuit fault then occurs at the beginning of loop II at 0.1 s. After the fault lasts 0.2 s, the fault line is removed, the generator rotor accelerates, and the system is unstable. At 0.314 s, the three-phase current of loop I is switched off simultaneously. The three-phase commutation sequence is then connected A to c, B to a, and C to b. The three-phase connected solid-state circuit breaker is switched on at 0.322 s to restore the three-phase current at the same time, and the phase sequence exchanging operation is completed. The wave of rotor speed, power angle, three-phase voltage, and current waveform are provided in Fig. 12(a), (b), (c), and (d), respectively.

As illustrated in Fig. 12(a), the rotor speed is accelerated from the short circuit to the phase sequence exchange. The phase sequence exchange is completed at 0.322 s, at which point the rotor begins to decelerate, and stabilizes at the rated speed after amplitude reduction oscillation.

As seen in Fig. 12(b), the power angle oscillates after the short circuit, but when the phase sequence exchange is completed at 0.322 s, the power angle is instantly pulled back from 177° to 57°. The power angle then stabilizes at 56° after amplitude reduction oscillation, and the system returns to stable operation.

Figure 12(c), shows the presence of a large three-phase impulse current in the phase sequence exchange. This is caused by unequal voltage at the two ends of the solid-state circuit breaker, resulting in activation impulse overcurrent. The current is then stabilized by three small fluctuations.

As illustrated in Fig. 12(d), an impulse overvoltage is generated due to the switching current of the solid state circuit breaker during phase sequence exchange, then the voltage oscillation attenuation tends to be stable.

Comparing Fig. 12 with Fig. 14, it can be observed that the single machine infinite bus system will cause system oscillation after a serious three-phase short circuit occurs at the generator side outlet bus. When the system is out of step, the application of PSET can effectively prevent the system from oscillating, and the rotor speed, power angle, three-phase voltage, and current tend to be stable after a short fluctuation. Therefore, PSET can return an oscillating system to a stable operation state and realize system stability control. At the same time, PSET produces impulse current and impulse voltage, and the impulse voltage produced by PSET is higher than that produced by a three-phase short circuit. Even if the system can be restrained from an out-of-step state, the system can not endure the impulse voltage generated by PSET.

The following section aims to reduce the impact of PSET by the method of split-phase switching control. In the simulation, a three-phase short circuit occurs at 0.1 s, and fault lines are removed at 0.3 s. The system starts to oscillate, and achieves the power angle threshold of PSET at 0.314 s. At the same time, the switch off instruction is issued. When the zero-crossing points of A, B, and C three-phase currents are monitored, the three-phase sequence is exchanged and A is connected to C, B is connected to a, and C is connected to b. The voltage at the two ends of the solid state circuit breaker connected to the three phases is then measured, and the solid state circuit breaker is closed when the voltage of both ends of the solid state circuit breaker is equal, finally completing phase sequence exchange. The wave of rotor speed, power angle, three-phase voltage, and current waveforms are shown in Fig. 13(a), (b), (c), and (d), respectively.

Comparing Fig. 12 and Fig. 13, it can be observed that the phase sequence exchange operation of two different control modes can stabilize the system. Wave comparison under two different control modes is provided in Fig. 14. Mode 1 is split-phase switching control, which is represented by the red line. Mode 2 is simultaneous switching control, which is represented by the blue line.

As illustrated in Fig. 14(a) and (b), although the effect of control mode 1 is slightly better, the changes of rotor speed and system power angle are essentially the same after PSET of different control modes at the same power angle position. This finding illustrates that power angle is the main factor determining the transient change after phase sequence exchange.

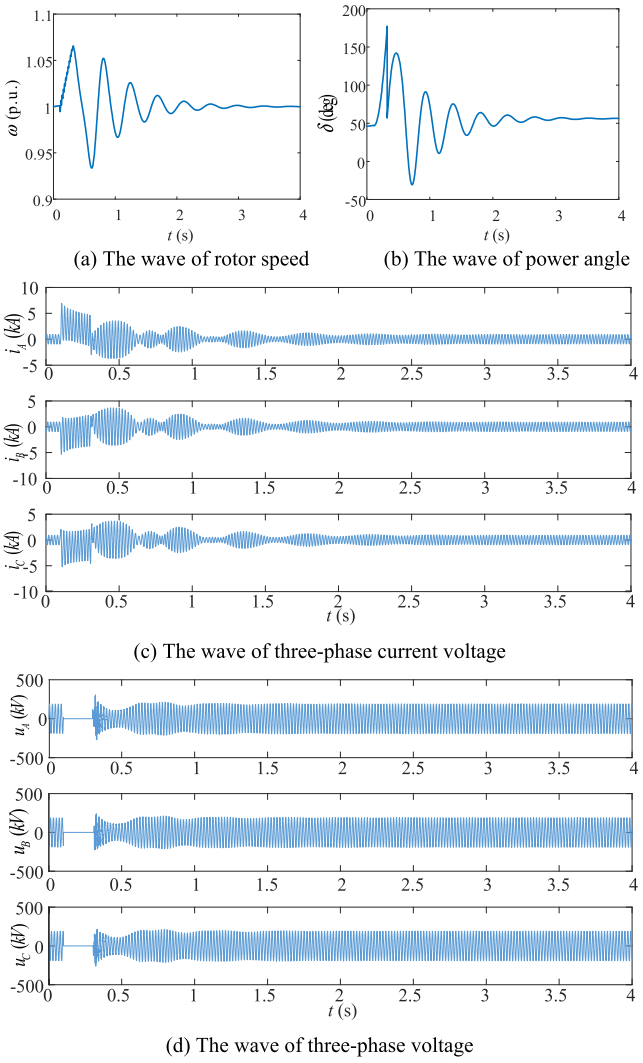

(a) The wave of rotor speed (b) The wave of power angle

(c) The wave of three-phase current voltage

(d) The wave of three-phase voltage

FIGURE 13. System simulation waveform with phase selection control method.

Figure 12(c) and (d) and Fig. 13(c) and (d) show that the impulse current produced by different control modes is essentially the same, but the impulse overvoltage is different. The maximum impulse overvoltage is as high as 2000 kV with simultaneous switching, while the maximum overvoltage is only 300 kV with split-phase switching. The lower overvoltage dramatically reduces the risk of system insulation breakdown and the voltage withstanding requirements of solid-state circuit breakers.

In the process of the PSET, the impact of the control mode of split-phase switching is minimal, which is beneficial to the stable operation of the system. At the same time, simultaneous switching has the advantages of simplicity, reliability, and economy. Considering the maximization of the effect of PSET, split-phase switching is preferable for the phase sequence exchange operation. When split-phase switching fails or emergency phase sequence exchange is required, the quick action speed of simultaneous switching can be used as a standby to provide double insurance for the PSET.

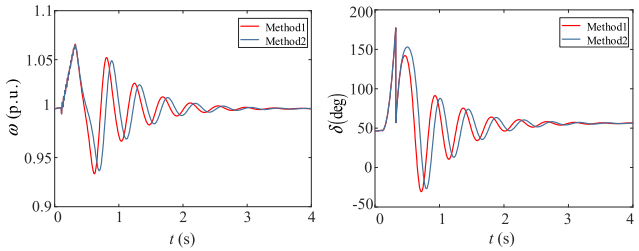

(a) The wave of rotor speed

(b) The wave of power angle

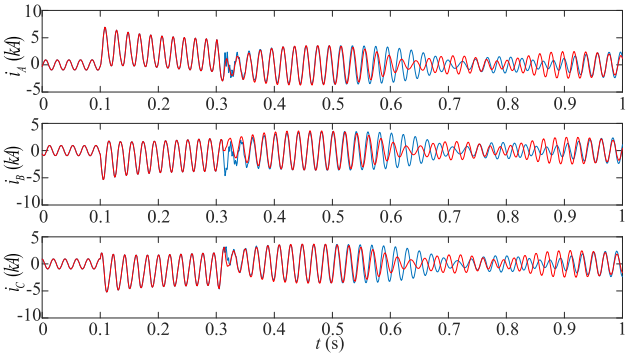

(c) The wave of three-phase current voltage

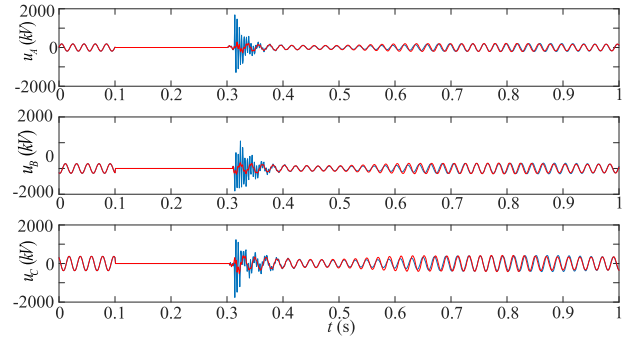

(d) The wave of three-phase voltage

FIGURE 14. **Wave comparison under two different control modes.**

VI. CONCLUSION AND FUTURE WORK

Phase sequence exchanging technology (PSET) is a recently developed emergency control technology for out-of-step power systems. The PSET system does not satisfy the condition of synchronization however, and will produce impulse current and impact torque.

In this paper, the impulse current and impact torque produced by PSET were calculated to be $0.52U/\left(X''_d + X_s\right)$ and $1.702/\left(X''_d + X_s\right)$, respectively. Taking the three-phase short circuit at the generator outlet as a reference, the impulse current generated by PSET was determined to be less than half of the three-phase short circuit at the generator outlet, which is within the system's endurable range. When the system satisfies $X_s/X''_d > 0.543$, it can withstand the impact torque produced by PSET. This finding is relevant for the practical application of PSET in order to directly determine whether the system can withstand the impact of phase sequence exchange.

To further reduce the impact of PSET on the system, a split-phase switching control method was proposed. Using this method, the system is shut off at the zero-crossing point of current and activated when two sides of the three-phase voltage are equal. An example was then provided which verified the effectiveness of the proposed control method.

As PSET is a recently developed emergency control technology, many theoretical and practical issues remain to be solved. The research and development of a phase sequence exchange device is a complex subject requiring design of the commutation sequence device itself (such a device has been proposed in previous papers which are under review). The impulse calculation and control strategy of phase sequence exchange must also be determined, as well as the installation position of the commutation sequence in the system. The acquisition and transmission of commutation sequence control signal are practical problems.

Application of the proposed control method was limited to Simulink simulation in this paper. Considering the financial and time cost of conducting a dynamic model test, this work will be conducted in the future when further conclusions are obtained from subsequent related studies.

REFERENCES

[1] S. Huang, Y. Li, H. Li, and Y. Huang, "A new technology applied to power system stability control: Phase sequence exchange technology," *IEEE Access*, vol. 7, pp. 93002–93009, 2019.

[2] Q. Xu, C. Kang, N. Zhang, Y. Ding, Q. Xia, R. Sun, and J. Xu, "A probabilistic method for determining grid-accommodable wind power capacity based on multiscenario system operation simulation," *IEEE Trans. Smart Grid*, vol. 7, no. 1, pp. 400–409, Jan. 2016.

[3] Z. Ma, C. Shen, F. Liu, and S. Mei, "Fast screening of vulnerable transmission lines in power grids: A pagerank-based approach," *IEEE Trans. Smart Grid*, vol. 10, no. 2, pp. 1982–1991, Mar. 2019.

[4] P. Dey, R. Mehra, F. Kazi, S. Wagh, and N. M. Singh, "Impact of topology on the propagation of cascading failure in power grid," *IEEE Trans. Smart Grid*, vol. 7, no. 4, pp. 1970–1978, Jul. 2016.

[5] J. Ma, S. Wang, Y. Qiu, Y. Li, Z. Wang, and J. S. Thorp, "Angle stability analysis of power system with multiple operating conditions considering cascading failure," *IEEE Trans. Power Syst.*, vol. 32, no. 2, pp. 873–882, Mar. 2017.

[6] W. Yu, Y. Xue, J. Luo, M. Ni, H. Tong, and T. Huang, "An UHV grid security and stability defense system: Considering the risk of power system communication," *IEEE Trans. Smart Grid*, vol. 7, no. 1, pp. 491–500, Jan. 2016.

[7] W. Du, Q. Fu, and H. F. Wang, "Power system small-signal angular stability affected by virtual synchronous generators," *IEEE Trans. Power Syst.*, vol. 34, no. 4, pp. 3209–3219, Jul. 2019.

[8] P. Bhui and N. Senroy, "Real-time prediction and control of transient stability using transient energy function," *IEEE Trans. Power Syst.*, vol. 32, no. 2, pp. 923–934, Mar. 2017.

[9] F. Milano, "On current and power injection models for angle and voltage stability analysis of power systems," *IEEE Trans. Power Syst.*, vol. 31, no. 3, pp. 2503–2504, May 2016.

[10] H. Bosetti and S. Khan, "Transient stability in oscillating multi-machine systems using Lyapunov vectors," *IEEE Trans. Power Syst.*, vol. 33, no. 2, pp. 2078–2086, Mar. 2018.

[11] R. G. D. Almeida, J. A. P. Lopes, and J. A. L. Barreiros, "Improving power system dynamic behavior through doubly fed induction machines controlled by static converter using fuzzy control," *IEEE Trans. Power Syst.*, vol. 19, no. 4, pp. 1942–1950, Nov. 2004.

[12] Z. Li, G. Yao, G. Geng, and Q. Jiang, "An efficient optimal control method for open-loop transient stability emergency control," *IEEE Trans. Power Syst.*, vol. 32, no. 4, pp. 2704–2713, Jul. 2017.

[13] A. G. Beccuti, T. H. Demiray, G. Andersson, and M. Morari, "A lagrangian decomposition algorithm for optimal emergency voltage control," *IEEE Trans. Power Syst.*, vol. 25, no. 4, pp. 1769–1779, Nov. 2010.

[14] T. Cui, W. Lin, Y. Sun, J. Xu, and H. Zhang, "Excitation voltage control for emergency frequency regulation of island power systems with voltage-dependent loads," *IEEE Trans. Power Syst.*, vol. 31, no. 2, pp. 1204–1217, Mar. 2016.
[15] J. Cao, W. Du, H. Wang, Z. Chen, and H. F. Li, "A novel emergency damping control to suppress power system inter-area oscillations," *IEEE Trans. Power Syst.*, vol. 28, no. 3, pp. 3165–3173, Aug. 2013.
[16] S. R. Islam, D. Sutanto, and K. M. Muttaqi, "A distributed multi-agent based emergency control approach following catastrophic disturbances in interconnected power systems," *IEEE Trans. Power Syst.*, vol. 31, no. 4, pp. 2764–2775, Jul. 2016.
[17] G. Gan, Z. Zhu, G. Geng, and Q. Jiang, "An efficient parallel sequential approach for transient stability emergency control of large-scale power system," *IEEE Trans. Power Syst.*, vol. 33, no. 6, pp. 5854–5864, Nov. 2018.
[18] D. Ruiz-Vega and M. Pavella, "A comprehensive approach to transient stability control. I. Near optimal preventive control," *IEEE Trans. Power Syst.*, vol. 18, no. 4, pp. 1446–1453, Nov. 2003.
[19] K. M. J. Rahman, M. M. Munnee, and S. Khan, "Largest blackouts around the world: Trends and data analyses," in *Proc. IEEE Int. WIE Conf. Elect. Comput. Eng. (WIECON-ECE)*, Pune, India, Dec. 2016, pp. 155–159.
[20] Y. Song, D. J. Hill, and T. Liu, "Static voltage stability analysis of distribution systems based on network-load admittance ratio," *IEEE Trans. Power Syst.*, vol. 34, no. 3, pp. 2270–2280, May 2019.
[21] M. H. Haque, "Improvement of first swing stability limit by utilizing full benefit of shunt FACTS devices," *IEEE Trans. Power Syst.*, vol. 19, no. 4, pp. 1894–1902, Nov. 2004.
[22] Z. Li, Q. Guo, H. Sun, and J. Wang, "Impact of coupled transmission-distribution on static voltage stability assessment," *IEEE Trans. Power Syst.*, vol. 32, no. 4, pp. 3311–3312, Jul. 2017.
[23] H. Tao, C. Kuai, Y. Zi-De, W. Jia-Liang, and W. Jun, "The researches on adaptive synchronized grid-connected of small generator," in *Proc. 4th Int. Conf. Electr. Utility Deregulation Restructuring Power Technol. (DRPT)*, Weihai, China, Jul. 2011, pp. 951–954.
[24] Y. P. Bhatt and M. C. Shah, "Design, analysis and simulation of synchronous reference frame based phase lock loop for grid connected inverter," in *Proc. IEEE 1st Int. Conf. Power Electron., Intell. Control Energy Syst. (ICPEICES)*, New Delhi, India, Jul. 2016, pp. 1–5.
[25] Y. Yang, K. Zhou, and F. Blaabjerg, "Enhancing the frequency adaptability of periodic current controllers with a fixed sampling rate for grid-connected power converters," *IEEE Trans. Power Electron.*, vol. 31, no. 10, pp. 7273–7285, Oct. 2016.
[26] S. S, and L. Umanand, "A unified controller for utility-interactive uninterruptible power converters for grid connected and autonomous operations," *IEEE Trans. Power Electron.*, vol. 34, no. 4, pp. 3871–3887, Apr. 2019.
[27] N. T. Stringer, "Voltage considerations during generator synchronizing," *IEEE Trans. Ind. Appl.*, vol. 35, no. 3, pp. 526–529, May 1999.
[28] O. D. Momoh, S. J. Loeffler, N. J. Dykhuizen, I. Hack, and G. D. Steffen, "LabVIEW based automatic paralleling of synchronous generator system," in *Proc. 44th Southeastern Symp. Syst. Theory (SSST)*, Jacksonville, FL, USA, Mar. 2012, pp. 204–208.
[29] T.-H. Tseng, P.-H. Huang, and Y.-H. Chang, "Analysis of effects of synchronism conditions on power system operation," in *Proc. SICE Annu. Conf.*, Tokyo, Japan, Sep. 2011, pp. 1416–1419.
[30] Y. Zhou, J. A. Ferreira, and P. Bauer, "Grid-connected and islanded operation of a hybrid power system," in *Proc. IEEE Power Eng. Soc. Conf. Expo. Afr.-PowerAfrica*, Johannesburg, South Africa, Jul. 2007, pp. 1–6.
[31] H. Nian and Y. Song, "Direct power control of doubly fed induction generator under distorted grid voltage," *IEEE Trans. Power Electron.*, vol. 29, no. 2, pp. 894–905, Feb. 2014.
[32] J. Li, G. Konstantinou, H. R. Wickramasinghe, J. Pou, X. Wu, and X. Jin, "Impact of circulating current control in capacitor voltage ripples of modular multilevel converters under grid imbalances," *IEEE Trans. Power Del.*, vol. 33, no. 3, pp. 1257–1267, Jun. 2018.
[33] Y. Pan, M. Steurer, T. L. Baldwin, and P. G. McLaren, "Impact of waveform distorting fault current limiters on previously installed overcurrent relays," *IEEE Trans. Power Del.*, vol. 23, no. 3, pp. 1310–1318, Jul. 2008.
[34] Y. Wang, S. G. Abdulsalam, and W. Xu, "Analytical formula to estimate the maximum inrush current," *IEEE Trans. Power Del.*, vol. 23, no. 2, pp. 1266–1268, Apr. 2008.
[35] S. Kamtip and K. Bhumkittipich, "Comparison between mechanical circuit breaker and solid state circuit breaker under abnormal conditions for low voltage systems," in *Proc. 18th Int. Conf. Electr. Mach. Syst. (ICEMS)*, Pattaya, Thailand, Oct. 2015, pp. 1091–1096.
[36] R. K. Smith, P. G. Slade, M. Sarkozi, E. J. Stacey, J. J. Bonk, and H. Mehta, "Solid-state distribution current limiter and circuit breaker: Application requirements and control strategies," *IEEE Trans. Power Del.*, vol. 8, no. 3, pp. 1155–1164, Jul. 1993.
[37] S. M. Wong, L. A. Snider, and E. W. C. Lo, "Overvoltages and reignition behavior of vacuum circuit breaker," in *Proc. 6th Int. Conf. Adv. Power Syst. Control, Oper. Manage. (ASDCOM)*, 2003, pp. 653–658.
[38] R. P. P. Smeets, A. G. A. Lathouwers, and L. H. te Paske, "Testing of vacuum circuit breakers: Specific issues and developments," in *Proc. 5th Int. Conf. Trends Distrib. Switchgear, 400V-145kV Utilities Private Netw.*, London, U.K., Nov. 1998, pp. 149–154.
[39] P.-A. Lof, T. Smed, G. Andersson, and D. J. Hill, "Fast calculation of a voltage stability index," *IEEE Trans. Power Syst.*, vol. 7, no. 1, pp. 54–64, Feb. 1992.

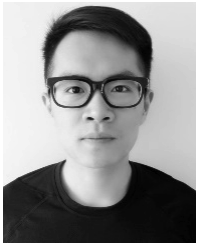

YIFAN LI was born in Shandong, China, in 1994. He received the B.S. degree in electrical engineering from North China Electric Power University (NCEPU), in 2016. He is currently pursuing the Ph.D. degree in electrical engineering with the State Key Laboratory for Alternate Electrical Power System With Renewable Energy Sources, North China Electric Power University. His research interests include power system emergency control and transient stability.

SHAOFENG HUANG (M'08) was born in Fujian, China, in 1958. He received the bachelor's degree in electrical engineering from North China Electric Power University, Baoding, China, in 1982. He is currently a Professor with the Electrical Engineering Department, North China Electric Power University. His research interests include power system automation and protection.

HUI LI was born in Shandong, China, in 1994. She received the B.S. degree in electrical engineering from North China Electric Power University, Beijing, China, in 2016, where she is currently pursuing the Ph.D. degree. Her main research interest focuses on stability analysis of power system.

JIAN ZHANG was born in Anhui, China, in 1996. He received the bachelor's degree in electrical engineering and automation from North China Electric Power University, in 2018, where he is currently pursuing the master's degree in electrical engineering. His main research interest includes stability analysis of power system.

GANG HUANG was born in Jiangxi, China, in 1994. He received the bachelor's degree in electrical engineering and automation from North China Electric Power University, in 2017, where he is currently pursuing the master's degree in electrical engineering. His research interest includes stability analysis of power system and power electronic device.

YANGJINGYI LUO was born in Chongqing, China, in 1994. He received the bachelor's degree in electrical engineering from Northeast Electric Power University, in 2017. He is currently pursuing the master's degree in electrical engineering with North China Electric Power University. His research interest includes solid state circuit breaker.